

Study of delamination in REBCO coated conductor by transmission electron microscopy

Yan Xin, Jun Lu, and Ke Han

Abstract— Delamination strength of REBCO is very important for its applications in large magnet projects. This work presented the transmission electron microscopy (TEM) investigation of the microstructures of the REBCO coated conductor to understand its delamination property. We found that the low delamination strength is associated with nano-voids formed at the IBAD MgO/Y₂O₃ interface.

Index Terms— Delamination, REBCO Coated Conductor tape, TEM, Microstructures.

I. INTRODUCTION

The second generation high temperature superconductor (HTS) rare-earth-barium-copper-oxide REBCO tapes are excellent conductor for building ultrahigh field superconducting magnets [1], [2]. REBCO are typically grown on ion beam assisted deposited (IBAD) buffer layers on Hastelloy® C-276 polished substrates [3]. There have been a few property issues in its application, among which is the delamination of REBCO's layered structure that degrade the critical currents. The delamination might happen due to the handling during the coil fabrication, due to thermal stress during magnet cool down, and due to the electromagnetic forces during operation [4]. Therefore, the toughness of REBCO against delamination is very important. There are a number of studies transverse mechanical strength using different methods, such as peeling test, the double cantilever beam method, climbing drum test, and anvil mechanical test [5-9]. The location of delamination are found to be inside the REBCO layer, between REBCO layer and the buffer, within the buffer stack, or between Ag/REBCO top surface, and in mixed fashion [10-12].

Understanding why the delamination occurs at particular interfaces and identifying the underlying cause of a weak interface is essential to improve the transverse mechanical strength. There have been very few high resolution microstructures characterization to study the cause of delamination, and identify the delaminating interface. Therefore, in this work, we study the interfaces of REBCO multilayered structure using various transmission electron microscopy (TEM) techniques, with specific focus on the possible delaminating interfaces. With the detailed

microstructure analysis and comparison of REBCO samples of the weak and strong peel strength, we reveal weak interface and the possible causes of it.

II. EXPERIMENTALS

REBCO samples are made at SuperPower Inc. by the IBAD/MOCVD method grown on Hastelloy C-276 substrate. Its layer structure is depicted in Fig. 1 (not to scale).

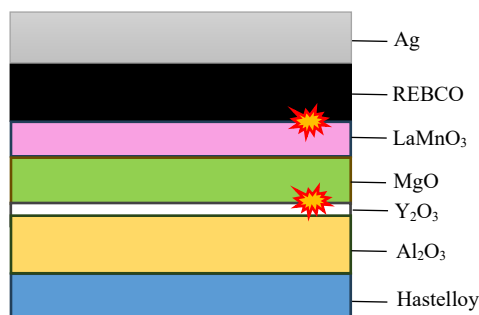


Fig. 1. a schematic of layer structure of SuperPower REBCO tape. The possible delamination interfaces are indicated.

The tape is 4 mm wide with 20 μm electroplated copper. As part of the incoming material quality assurance for the 40 T all-superconducting magnet project at the National High Magnetic Field Laboratory, the delamination strength of REBCO are tested for every 100 – 200 m piece length by 90 degree peel strength at room temperature [13]. In this work, we study the interfacial microstructure of a sample that has a peel strength of 1.02 N/cm (strong tape) and a sample with peel strength of only 0.12 N/cm (weak tape).

The cross-sectional TEM samples were prepared by focused ion beam (FIB) on a Helios G4 scanning electron microscope (SEM). The microstructures of the tapes were studied by scanning transmission electron microscopy (STEM) using the probe-aberration-corrected JEOL JEM-ARM200cF at 200 kV. High-angle annular scanning transmission electron microscopy (HAADF-STEM) imaging and the annual-bright-field STEM (ABF-STEM) imaging were the two major imaging techniques used. Electron energy loss spectroscopy (EELS) and energy dispersive X-ray spectroscopy (EDS) spectrum imaging (SI) were used in STEM mode with a probe size of 0.11 nm using Gatan GIF and Oxford Aztec EDS detector.

This work was performed at the National High Magnetic Field Laboratory, which is supported by the National Science Foundation Cooperative Agreement No. DMR-1644779, DMR-1839796, DMR- 2131790, and the State of Florida. (Corresponding author: Yan Xin and Jun Lu.)

Yan Xin, Jun Lu, and Ke Han are with Magnet Science and Technology

division at National High Magnetic Laboratory, Tallahassee, FL 32310 USA (e-mail: xin@magnet.fsu.edu; junlu@magnet.fsu.edu; han@magnet.fsu.edu).

Color versions of one or more of the figures in this article are available online at <http://ieeexplore.ieee.org>

III. RESULTS

A. The surface of the weak tape after delamination

After the 90 degree peel test, it was observed that both sides of the delaminated strong tape showed black color. This indicates that delamination occurred within the REBCO layer which is black. In contrast, the weak tape delaminated within the buffer stack manifested by the yellowish color on the substrate side of the delaminated tape. The yellowish color comes from the interference of the lights reflected from different interfaces of the buffer stack which is transparent.

As shown in Fig. 2(a), the weak tape was peeled leaving the superconductor layer (black) attached to the copper side. The substrate side showing yellow color for most area, with small patches of teal blue. To determine the delaminated surfaces of both yellow and blue areas, we used FIB to cut a TEM lamella that includes both regions as indicated in the inset of Fig. 2 (b). The SEM cross-sectional view of the TEM sample is shown in Fig. 2 (b) indicate more buffer layers remain on the blue color area than the yellow color area. The elemental EDS maps (Fig. 2 (c) to (h)) revealed that the surface for the yellow area is Y_2O_3 and the blue area is $LaMnO_3$ (LMO). The cross-sectional STEM view of the intersection between yellow and blue areas is shown in Fig. 2 (j). The further magnified image Fig. 2(k) indicates reasonable bonding between MgO lattice planes and those of the Y_2O_3 grains, which suggest that the MgO/ Y_2O_3 interface at this boundary is relatively strong, and the weaker link is at the REBCO/LMO interface instead. This is why the delamination occurred at REBCO/LMO interface at this point, leaving a patch of LMO layer (blue) at the surface. However, Fig. 2 (j) also reveals nanometer sized voids at MgO/ Y_2O_3 interface. The detailed microanalysis of these nano voids will be presented in section III C.

B. The REBCO/ $LaMnO_3$ interface

The results shown in Fig. 2 suggests that both REBCO/LMO and MgO/ Y_2O_3 interfaces are possible delamination locations. To compare the REBCO/LMO interface of the strong and weak tapes, a cross-sectional TEM sample was cut in width direction for each of the as-received tapes. Fig. 3(a) and (b) are ABF-STEM images that show REBCO/LMO interfaces of the strong and the weak tape respectively. The darker contrast at interface of the weak tape (Fig. 3(b)) suggests interfacial strain. The HAADF-STEM images in Fig. 3(c) (strong tape) and 3(e) (weak tape) are not significantly different. Both show good epitaxial relationships of REBCO/LMO with the atomic planes across the REBCO/LMO interface. Further analysis is performed by inverse FFT where REBCO(006)/LMO(101) spots, indicated by red circles in the inset of Fig. 3 (d) and (f), are used to obtain the inverse FFT images (Fig. 3(d) and (f)). They show that the strong tape has coherent interface, whereas the weak tape has two extra atomic planes as labelled by the red lines and red arrows in Fig. 3(f). The extra atomic planes is indicative of interfacial edge dislocations which might be one of the reasons for delamination at REBCO/LMO interface.

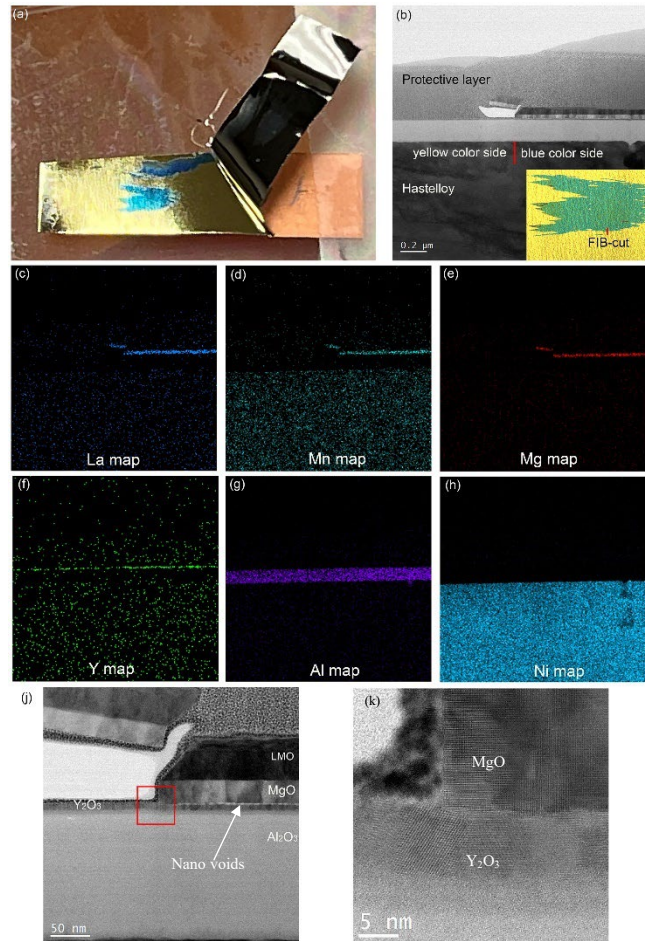


Fig. 2. (a) a picture of the delaminated weak tape. (b) ABF-STEM image of the cross-sectional view at the yellow/blue boundary. Inset: a picture of the blue patch. (c) to (h) elemental EDS maps. (j) and (k) high resolution ABF-STEM image of cross-sectional view of the joint at the yellow/blue boundary. (k) higher magnification image of the red box in (j)

C. MgO/ Y_2O_3 interface

Based on the observations presented in section III A, the delamination of the weak tape mostly occurs at the MgO/ Y_2O_3 interface. Therefore, we examine this interface of both samples for comparison. The MgO/ Y_2O_3 interface of both strong and weak tapes as shown in Fig. 4. Compared to the MgO/ Y_2O_3 interface of the strong tape (Fig.4(a)), this interface of the weak tape shows a contrast of a bright band in the TEM bright field (BF) image (Fig.4(b))

To accurately image the interfaces without delocalization effect of BF-TEM, ABF-STEM was used, and results are shown in Fig. 4(c) and 4(d). Compared to the smaller and more separated bright area at the MgO/ Y_2O_3 interface of the strong tape (Fig. 4(c)), the band in the weak tape is wider and brighter (Fig. 4(d)) indicating less material at the interface. The corresponding HAADF-STEM images (Fig. 4(e) and 4(f)) also show darker contrast at this interface. It is well known that the intensity of HAADF-STEM image is proportional to $Z^{1.7}$ (Z is atomic number of the element) as well as sample thickness along the electron beam direction [14]. Since atomic number of

1J-ML-Or1A-05

Y is much greater than Mg and Al, Y_2O_3 layer shows brighter contrast than MgO and Al_2O_3 layer. The dark contrast at the interface corresponds to nano-voids which results in less thickness along the electron beam direction. Apparently, the interfacial nano-voids are larger and closer together in the weak tape (Fig. 4(f)). The average dimension of the nano-voids is about $3\text{ nm} \times 2\text{ nm}$ for the strong tape, and $5\text{ nm} \times 2.5\text{ nm}$ for the weak tape. Their dimensions in the depth direction (perpendicular to the paper) will be discussed below in junction with Fig. 5.

On closer examination of the MgO/Y_2O_3 interface of the weak sample (Fig. 5(a) and (b)), it is discernable that the Y_2O_3 layer is comprised of three regions: R1, nano-void region of about 2 nm just below the MgO layer; R2, the crystalline Y_2O_3 region of about 7 nm; and R3, the amorphous region of 4 nm of Y_xAl_yO which is the intermixture of Y_2O_3 and the Al_2O_3 layer below. The strong tape has similar microstructural morphology except the R1 region. Along the MgO/Y_2O_3 interface at different location, the nano-voids appears to have different shape and sizes, as shown in Fig. 5(c) and (d).

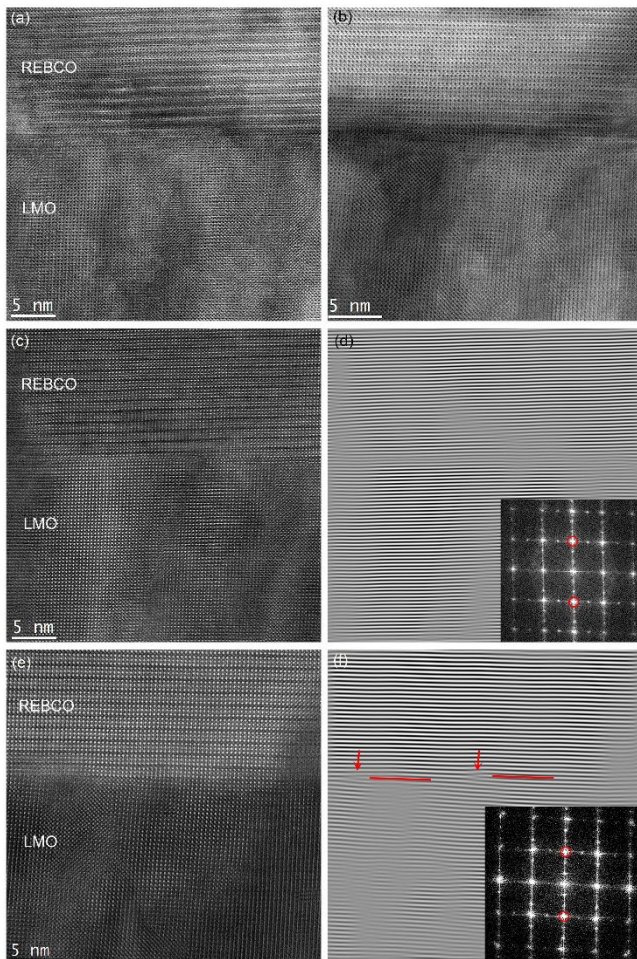


Fig. 3. (a) ABF-STEM image of the REBCO/LMO interface of a strong tape. (b) ABF-STEM image of the REBCO/LMO interface of a weak tape. (c) Corresponding HAADF-STEM image of (a). (d) Inverse FFT of (c). inset: FFT diffraction pattern. (e) Corresponding HAADF-STEM image of (b). (f) Inverse FFT of (e). inset: FFT diffraction pattern.

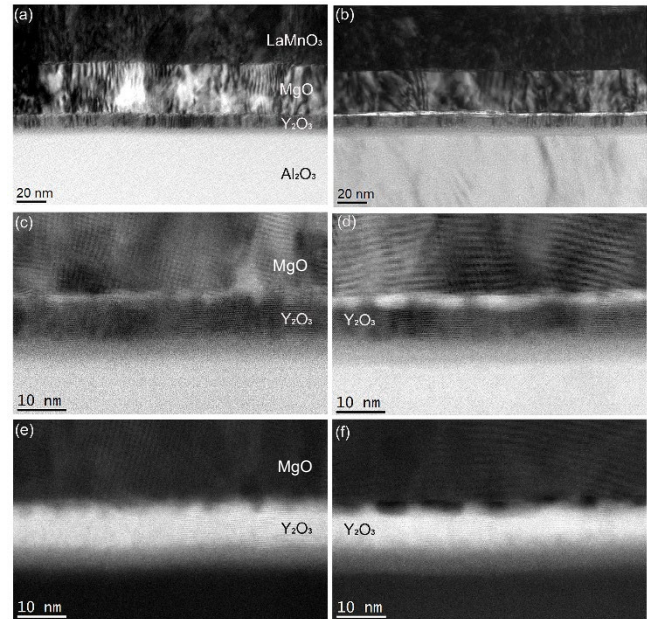


Fig. 4. General cross-sectional view of the MgO/Y_2O_3 interface of both strong and weak tape. (a) TEM BF image of the strong tape. (b) TEM BF image of the weak tape. (c)-(d) ABF-STEM images of the strong tape. (e)-(f) HAADF-STEM images of the weak tape.

In order to measure the depth of the nano-voids, we collected the EELS spectra from the interfacial region of both samples. and used EELS log-ratio method to obtain the thickness map of this region. Fig. 5(e) shows a region (red box) of the weak sample where EELS spectra are taken. Fig. 5(f) the thickness map (by EEL-spectra imaging) corresponding to the red box region. The measured depths of Y_2O_3 at these voids are 20 – 25 nm out of total of 38 nm. Therefore, the size of the void in depth direction is 13 – 15 nm (about 34 – 39% of total). It should be noted that this 13-15 nm corresponds to one or more voids in the depth direction. In comparison, the depth of voids in the strong tape is only 7 nm out of total of 65 nm (11%).

It is important to verify whether the interfacial voids are results of contamination in the deposition process. The elemental EDS maps of the weak tape are shown in Fig. 6 where no contaminating elements, typically carbon, are segregated at the MgO/Y_2O_3 interface, although the Y_2O_3 layer has a small amount of carbon distributed through the entire layer. Moreover, the EDS spectrum taken from the interface region (the box in Fig 6(a)) is shown in Fig. 6 (g). Again, no significant amount of contaminating was detected except Ar which seem to exist in the entire Y_2O_3 layer.

1J-ML-Or1A-05

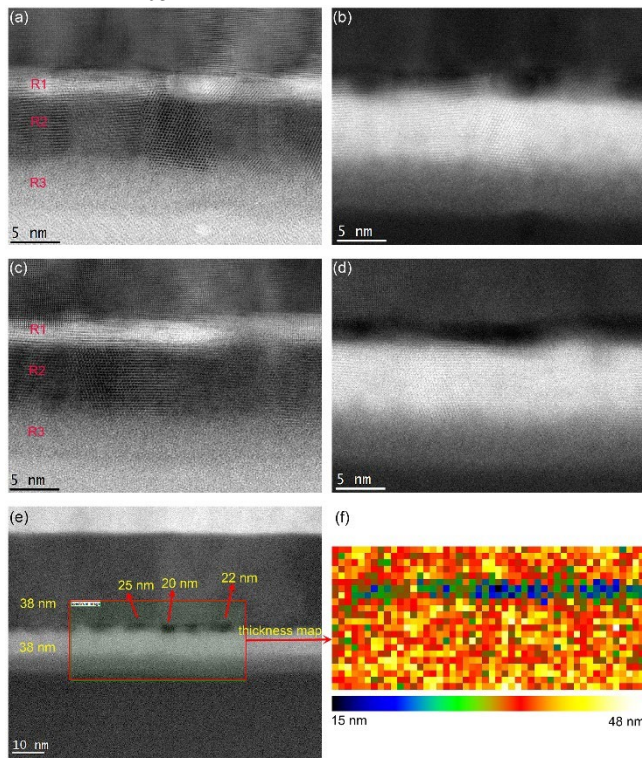


Fig. 5. Atomic resolution images of the MgO/Y₂O₃ interfaces of the weak tape. (a) and (b) a pair of ABF-STEM and HAADF-STEM images of one region of the interface. (c) and (d) a pair of ABF-STEM and HAADF-STEM images of another region of the interface. (e) The interface region where the EEL-Spectra Image was collected. (f) The thickness map of the region.

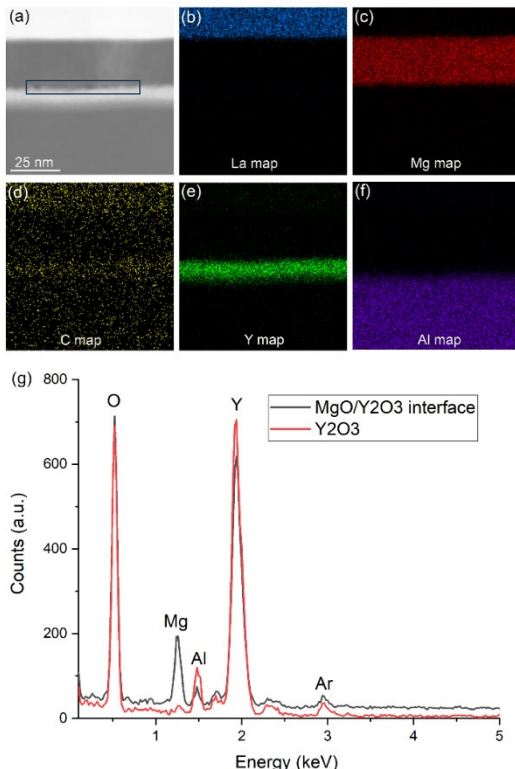


Fig. 6. Elemental EDS maps: (a)STEM image of mapped region; (b) La map; (c) Mg map; (d) C map; (e) Y map; (f) Al map. (g) EDS spectra from the MgO/Y₂O₃ interface (black) and from the middle of Y₂O₃ layer (red).

IV. DISCUSSIONS

Our microscopy analysis clearly shows that the high density nano-voids at the MgO/Y₂O₃ interface is responsible for the low delamination strength of the weak sample. We have noticed that these nano-voids are present in both samples, and not uniformly distributed. The higher fraction of nano-voids at the interface, the weaker delamination strength of the tape.

We speculate that these nano-voids originated during the IBAD MgO growth. In the IBAD process, Ar ion beam bombards the Y₂O₃ surface while the MgO is growing by magnetron sputtering or by thermal evaporation. When the parameters of the Ar ion beam deviates from its optimal conditions, it might result in a relatively rough MgO/Y₂O₃ interface. During the subsequent REBCO growth at higher temperature, the amorphous Y₂O₃ layer turns into crystalline, turning the rough interface into nano-voids at the interface.

Our investigation (not presented here) also shows that the crystal quality of the superconductor layer of both strong and weak tapes are similar. Consequently, their superconducting properties are similar, as confirmed by their critical current (I_c) measured at 77 K self-field. Therefore, it seems that nano-voids at the MgO/Y₂O₃ interface of the weak sample do not compromise the crystal quality and the electrical performance of REBCO.

V. CONCLUSION

Delamination strength of REBCO is very important for its applications in large magnet projects. To identify the layer location of the delamination, we studied the interfaces of SuperPower REBCO tapes that show strong and weak peel strength by transmission electron microscopy techniques. We found nano-voids at the IBAD MgO/Y₂O₃ interface which is likely the cause of the weak peel strength. Dislocations at the REBCO/LaMnO₃ interface added unwanted stress and might have contributed to weakening REBCO/LMO interface.

REFERENCES

- [1] H. W. Weijers, et al., 'Progress in the Development and Construction of a 32-T Superconducting Magnet' *IEEE Trans. Appl. Supercond.*, vol. 26, no. 4, 2016, Art. no. 4300807.
- [2] H. Bai, M.D. Bird, L. Cooley, I.R. Dixon, K.L. Kim, D.C. Larbalestier, W.S. Marshall, U.P. Trociewitz, H.W. Weijers, D.V. Abramov, G.S. Boebinger, "The 40 T Superconducting Magnet Project at the National High Magnetic Field Laboratory," *IEEE Transactions on Applied Superconductivity*, vol. 30, no. 4, pp. 1-5, Jan. 2020, doi: 10.1109/TASC.2020.2969642.
- [3] Y. Zhang, T. F. Lehner, T. Fukushima, H. Sakamoto, and D. W. Hazelton, "Progress in Production and Performance of Second Generation (2G) HTS Wire for Practical Applications," *IEEE Transactions on Applied Superconductivity*, vol. 24, No. 5, pp. 7500405, Oct. 2014, doi: 10.1109/TASC.2014.2340458.
- [4] T. Takematsu, R. Hu, T. Takao, Y. Yanagisawa, H. Nakagome, D. Uglietti, T. Kiyoshi, M. Takahashi, H. Maeda, "Degradation of the performance of

1J-ML-Or1A-05

- a YBCO-coated conductor double pancake coil due to epoxy impregnation”, *Physica C: Superconductivity and its Applications*, vol. 470, No. 17-18, pp. 674677, Sept. 2010, doi: 10.1016/j.physc.2010.06.009.
- [5] Y. Zhang, D.W. Hazelton, A.R. Knoll, J.M. Duval, P. Brownsey, S. Repnoy, S. Soloveichik, A. Sundaram, R.B. McClure, G. Majkic, and V. Selvamanickam, “Adhesion strength study of IBAD–MOCVD-based 2G HTS wire using a peel test,” *Physica C: Superconductivity*, vol. 473, pp. 41-47, Feb. 2012, doi: 10.1016/j.physc.2011.11.013.
- [6] T. Miyazato, M. Hojo, M. Sugano, T. Adachi, Y. Inoue, K. Shikimachi, N. Hirano, and S. Nagaya., “Mode I type delamination fracture toughness of YBCO coated conductor with additional Cu layer,” *Physica C: Superconductivity and its Applications*, vol. 471, No. 21-22, pp. 1071-1074, Nov. 2011, doi: 10.1016/j.physc.2011.05.126.
- [7] N. J. Long, R. C. Mataira, E. Talantsev and R. A. Badcock, " Mode I Delamination Testing of REBCO Coated Conductors via Climbing Drum Peel Test," *IEEE Transactions on Applied Superconductivity*, vol. 28, no. 4, pp. 1-5, June 2018, Art no. 6600705, doi: 10.1109/TASC.2018.2791514.
- [8] D. C. van der Laan, J. W. Ekin, C. C. Clickner and T. C. Stauffer, “Delamination strength of YBCO coated conductors under transverse tensile stress,” *Supercond. Sci. Technol.*, vol. 20, No. 8, pp. 765-770, Jun. 2007, doi: 10.1088/0953-2048/20/8/007.
- [9] A. Gorospe, A. Nisay, J.R. Dizon, H.S. Shin, “Delamination behaviour of GdBCO coated conductor tapes under transverse tension,” *Physica C: Superconductivity*, vol. 494, pp. 163-167, Feb. 2012, doi: 10.1016/j.physc.2011.11.013.
- [10] I. Kesgin, N. Khatri, Y. Liu, L. Delgado, E. Galstyan, V. Selvamanickam , “Influence of superconductor film composition on adhesion strength of coated conductors”, *Supercond. Sci. Technol.*, vol. 29, No. 1, pp. 015003(10pp), Jan. 2016, doi: 10.1088/0953-2048/29/1/015003.
- [11] A. Gorospe, H.S. Shin, “Characterization of transverse tensile stress response of critical current and delamination behaviour in GdBCO coated conductor tapes by anvil test,” *Supercond. Sci. Technol.*, vol. 27, No. 8, pp. 025001 (13pp), Jan. 2014, doi: 10.1088/09532048/27/2/025001.
- [12]H.S. Shin, “Evaluation of delamination characteristics in GdBCO CC tapes under transverse load using anvil test methods for various anvil contact configurations at 77K”, *Supercond. Sci. Technol.*, vol. 32, No. 10, pp. 104001 (10pp), Aug. 2019, doi: 10.1088/1361-6668/ab3151.
- [13]J. Lu, et al., ‘2MPo2C-01: REBCO delamination characterization by 90 degree peel test’, in ASC-2024, Salt Lake City, UT, Sept. 1-6, 2024.
- [14]S. J. Pennycook, L. Boatner, “Chemically sensitive structure-imaging with a scanning transmission electron microscope”, *Nature*, vol. 336, pp. 565–567, Aug. 1988. <https://doi.org/10.1038/336565a0>